Wet deposition at the base of Mt Everest: Seasonal evolution of the chemistry and isotopic composition

Raffaella Balestrini [a, *], Carlo A. Delconte [a], Elisa Sacchi [b], Alana M. Wilson [c], Mark W. Williams [c], Paolo Cristofanelli [d], Davide Putero [d]

[a] CNR-IRSA − Water Research Institute, Brugherio, MB, Italy
[b] Department of Earth and Environmental Sciences, University of Pavia, Pavia, Italy
[c] Institute of Arctic and Alpine Research, University of Colorado at Boulder, USA
[d] CNR-ISAC—Institute for Atmospheric Sciences and Climate, Bologna, Italy

HIGHLIGHTS

- The chemical and isotopic composition of precipitation showed differences between rain and snow.
- Combustion emission tracers increased during the pre-monsoon and during the summer monsoon onset.
- Volume-weighted mean concentrations of SO_4^{2-} and NO_3^- did not differ from those measured in the 1990's.
- Ion deposition from snow largely contributed to the wet deposition fluxes.

ARTICLE INFO

ABSTRACT

The chemistry of wet deposition was investigated during 2012−2014 at the Pyramid International Laboratory in the Upper Khumbu Valley, Nepal, at 5050 m a.s.l., within the Global Atmosphere Watch (GAW) programme. The main hydro-chemical species and stable isotopes of the water molecule were determined for monsoon rain (July−September) and snow samples (October−June). To evaluate the synoptic-scale variability of air masses reaching the measurement site, 5 day back-trajectories were computed for the sampling period. Ion concentrations in precipitation during the monsoon were low suggesting that they represent global regional background concentrations. The associations between ions suggested that the principal sources of chemical species were marine aerosols, rock and soil dust, and fossil fuel combustion. Most chemical species exhibited a pattern during the monsoon, with maxima at the beginning and at the end of the season, partially correlated with the precipitation amount. Snow samples exhibited significantly higher concentrations of chemical species, compared to the monsoon rainfall observations. Particularly during 2013, elevated concentrations of NO_3^-, SO_4^{2-} and NH_4^+ were measured in the first winter snow event, and in May at the end of the pre-monsoon season. The analysis of large-scale circulation and wind regimes as well as atmospheric composition observations in the region indicates the transport of polluted air masses from the Himalayan foothills and Indian sub-continent up to the Himalaya region. During the summer monsoon onset period, the greater values of pollutants can be attributed to air-mass transport from the planetary boundary layer (PBL) of the Indo-Gangetic plains. Isotopic data confirm that during the monsoon period, precipitation occurred from water vapor that originated from the Indian Ocean and the Bay of Bengal; by contrast during the non-monsoon period, an isotopic signature of more continental origin appeared, indicating that the higher recorded NO_3^- and SO_4^{2-} concentrations could be ascribed to a change in air circulation patterns. A comparison of recent monsoon deposition chemistry with data from the 1990's shows similar levels of contaminants in the rainfall. However, non-monsoon deposition can be significant, as it largely contributed to the ion wet deposition fluxes for all analyzed species in 2013.

* Corresponding author.
E-mail address: balestrini@irsa.cnr.it (R. Balestrini).

1. Introduction

High-elevation environments are perceived to be among the most pristine regions on Earth owing to their remote location and distance from emissions sources. The Himalayas host a unique range of ecosystems with a high degree of biodiversity (Mittermeier et al., 2005), but they are characterized by a fragility that makes the region highly sensitive to environmental changes. The glaciers and snowpack of these mountains serve as "water towers" (Immerzeel et al., 2010), and their meltwaters are a major source of water for some of the largest rivers of Asia: the Indus, Ganga, and Brahmaputra.

Long-range aeolian transport of dust and pollution threaten the relatively pristine high-alpine ecosystems. They also jeopardize the stability of glaciers and snowpack by lowering albedo and making them more vulnerable to melt. A considerable amount of mineral dust is systematically transported toward the Himalaya from the Tibetan Plateau and the arid areas of the Indo-Gangetic Plains (Duchi et al., 2014). The southern Himalayans region is seasonally reached by high level of ozone (O_3), black carbon (BC), and other aerosol particles (Cristofanelli et al., 2014), which constitute the so-called atmospheric brown clouds (ABC).

Pollution from industrial emissions in neighboring China and India can alter the chemical composition of rain in the Himalayas. Between 2000 and 2008, emissions of nitrogen oxides (NO_x) increased more than 50% in India and sulfur dioxide (SO_2) emissions increased more than 50% in China (Kurokawa et al., 2013). There is evidence that emissions regulations in China have stabilized SO_2 emissions there since 2006, while SO_2 emissions in India have continued to increase (Klimont et al., 2013). Measurements of the quality of precipitation and dry deposition in the Himalayas are infrequent and geographically sparse, and there remain open questions regarding contribution of contaminants in the alpine environment. Data that do exist primarily come from the Tibetan Plateau (Li et al., 2007; Xu et al., 2009; Zhang et al., 2003), where desert dust dominates atmospheric deposition. Snow and ice core data for the Everest region demonstrate that monsoon air masses are the predominant sources of deposition on the southern slopes of the eastern Himalayas (Marinoni et al., 2001; Valsecchi et al., 1999; Shrestha et al., 2002). Some studies highlight differences in the wet deposition chemistry during different stages of the summer monsoon in high Nepali Himalayan valleys (Balestrini et al., 2014; Shrestha et al., 2002), indicating the transition phases of the monsoon season are critical periods for a full understanding of wet deposition behavior.

In this context, the chemistry of wet deposition was investigated at the Pyramid International Laboratory (PIL) in the northernmost portion of the Khumbu Valley, at 5050 m asl, within the Global Atmosphere Watch (GAW) programme. The main hydro-chemical species and the stable isotopes of oxygen and deuterium were measured for summer monsoon precipitation (2012–2013) and winter snow (2013–2014). To evaluate the synoptic-scale variability of the air masses reaching the measurement site, 5- day back-trajectories were computed for the sampling period.

The aim of this study was to analyze daily, weekly, and seasonal variation in the concentration of wet deposition chemistry and to analyze depositional fluxes during the different seasons that characterize the Himalayan climate. The chemical analysis combined with isotope data and the description of large-scale circulation provide insights into both the long-range transport of man-made contamination and the different origins of the air masses.

Additionally, we compared these results to previous measurements collected in the early 1990's (Valsecchi et al., 1999) in order to evaluate potential for changes in the quality of wet deposition over time. Our analysis focus on solutes in precipitation and, to help interpret these results, aerosols observations from our research site are discussed when available.

2. Methods

2.1. Study area

The rain and snow samples were collected at the Pyramid International Laboratory (PIL; 5050 m a.s.l.; 27.959°N; 86.813°E) located in the Khumbu Valley in the Sagarmatha (Mt. Everest) National Park of Nepal. The Khumbu Valley extends in elevation from 2845 m to 8848 m at the summit of Mt. Everest and lies in a geologically complex transition zone between Nepal and Tibet. Here, a large-scale and low-angle fault, called the South Tibetan detachment, places unmetamorphosed Paleozoic sediments, which make up the numerous peaks that exceed 8000 m (e.g., Mount Everest and Lhotze), above high-grade gneisses and leucogranites.

The Pyramid International Laboratory, located in the Upper Khumbu Valley, is a multi-disciplinary and high altitude research center, founded by the Ev-K2-CNR Committee and the Nepal Academy of Science and Technology in 1990 (Baudo et al., 2007).

The majority of rainfall (90%) in the sampling area occurs from June to September (Salerno et al., 2015) during the monsoon season, whereas the winter season is relatively dry. Land cover surroundings of the PIL are composed of typical upper alpine herbaceous vegetation (UNEP/WCMC, 2008) and rocks. About 75% of the surface area of glaciers in the valley is located between 5000 m and 6500 m a.s.l. (Salerno et al., 2015). An automatic weather station installed near the PIL allows for hourly recording of meteorological parameters (temperature, relative humidity, atmospheric pressure, wind speed and direction, global radiation, total precipitation) according to WMO standards (Bertolani et al., 2000). In addition, in 2006, a permanent station for aerosol, ozone and halocarbon measurements was established on the top of a hill near the PIL (the Nepal Climate Observatory-Pyramid — NCO-P) (Bonasoni et al., 2008).

2.2. Sampling and analyses

Precipitation was collected for chemical and isotopic analysis in 2012, 2013 and 2014. Rain water was sampled during the 2012 and 2013 monsoon seasons (June–September) by means of a wet-only sampler (MTX, Bologna, Italy) equipped with a polyethylene vessel (30 cm i.d.). Sampling was on a daily basis for the main part of the monsoon season, usually starting at 9.00 a.m., from July to mid-August. Sampling was on a weekly basis at the beginning and at the end of the rainy period (June; mid-August - September). During the non-monsoon period (from October to May) we sampled snow events by using a polyethylene vessel (30 cm i.d.) inserted in a plastic tank driven into the ground. This precaution was necessary because of the wind blowing at PIL site.

All the sample volumes were measured gravimetrically at the Pyramid laboratory. Depending on the amount of available volume, samples were poured in different plastic bottles for chemical or water molecule isotope analysis. Aliquots for chemical analyses were stabilized with chloroform (Galloway et al., 1989), used for its properties as a bactericide. Bottles were stored in plastic bags and refrigerated (4 °C) until shipment to Italy.

The amount of rain and snow were calculated using volumes and the area of the samplers. Weekly millimeters of rain compared with those measured by the automatic weather station showed good agreement. Some discrepancies were observed for snow due to the precipitation scarcity and the occurrence of strong wind. Therefore, the amount measured by means of the polyethylene vessel sometimes exceeded those measured by the automatic

weather station.

Analyses were performed on filtered samples (0.45 mm) except for conductivity and pH analyses which were conducted on the same aliquot of unfiltered sample. Major anions (N-NO$_3^-$, SO$_4^{2-}$ and Cl$^-$) and cations (Na$^+$, K$^+$, Mg^{2+}, Ca^{2+}) were analyzed by suppressed ion chromatography (Dionex). An AS11-HC column (KOH 30 mM as eluent) and a 100 μL injection loop was used for anions, whilst a CS12A column (CH$_3$SO$_3$H 20 mM as eluent) and a 450 μL injection loop was used for cations.

Ammonium (N-NH$_4^+$) was measured colourimetrically (Perkin Elmer, UV–VIS Lambda25) using the indophenol-blue method. When the sample volume was not sufficient, we used data obtained from ion chromatography. Alkalinity, according to the available volume, was obtained by a two end point potentiometric titration with HCl 0.01 M. On a small set of samples (n = 12), the HCO$_3^-$ concentration was estimated by the difference between the total cations and anions, assuming that the CO$_3^{2-}$ concentration was negligible (pH < 6.4). The concentrations of carboxylic acids (HCOO$^-$, CH$_3$COO$^-$ and C$_2$O$_4^{2-}$) and methanesulfonic acid (MSA), measured in the rain sampled during 2007 and 2008, were below the detection limits (Balestrini et al., 2014). Therefore, we assume that the concentrations of ionic species other than those we measured in the current sample set were negligible.

The analytical detection limits are 5 μg L^{-1} for N-NH$_4^+$, Na$^+$, K$^+$ Mg^{2+}, Cl$^-$, SO$_4^{2-}$; 10 μg L^{-1} for Ca^{2+}; and 2.2 μg L^{-1} for N-NO$_3^-$.

Quality control procedures included: 1) internal quality control (control charts); 2) check of ion balance and comparison of the measured and calculated conductivity, assuming we analyzed all main constituents in the sample; 3) participation in the EMEP and WMO-GAW laboratory intercomparison studies (EMEP; WMO-GAW).

Annual deposition fluxes were based on the annual volume weighted average concentrations multiplied by the annual amount of rainfall. The nonparametric Mann–Whitney U test (Helsel and Hirsch, 2002), was used to evaluate if there was a statistical difference in the ion concentration between the monsoon and non-monsoon. The differences between chemical composition of rain from 1991, 1992, 2008, 2012, and 2013 were tested by the nonparametric Kruskal Wallis test (Helsel and Hirsch, 2002).

The isotopic composition of rain was measured on cumulative samples that were collected either daily or weekly (in the month of July and in the first week of August for 2012 and 2013). Daily precipitation data were weighted by amount to obtain weekly precipitation values. The isotopic compositions of snow samples, collected from January to May in 2013 and 2014, correspond instead to single meteoric events, as precipitation is discontinuous and often not sufficient for the analysis.

The δ^{18}O and δ^{2}H isotope ratios were determined by Wavelength-Scanned Cavity Ring-Down Spectroscopy (WS-CRDS) at the Institute of Arctic and Alpine Research, University of Colorado at Boulder, USA. These results are reported in the usual delta (δ) notation versus Vienna Standard Mean Ocean Water (VSMOW) and with uncertainties (2σ) of ±0.2‰ and ±1‰, respectively.

To evaluate the synoptic-scale variability of the air-masses reaching the measurement site, 5-d back-trajectories starting at NCO-P were computed every 6 h (at 00:00, 06:00, 12:00 and 18:00 UTC), using the Lagrangian analysis tool LAGRANTO (Wernli and Davies, 1997; Sprenger and Wernli, 2015). The model calculations were based on the 6-hourly operational analysis field of the ECMWF (European Centre for Medium-Range Weather Forecast). To partially compensate for uncertainties related to the absence of sub-grid scale processes (e.g. convection and turbulent diffusion) in LAGRANTO, and to evaluate the coherence of flow, 19 additional back-trajectories per day were computed, with endpoints shifted by ± 1° in latitude/longitude and in a range of ±50 hPa with respect to the measurement site location.

3. Results and discussion

3.1. Meteorological regime and large-scale circulation

The large-scale circulation patterns over the period of interest (2012–2014) for monsoon and non-monsoon seasons are shown in Fig. 1. During non-monsoon seasons (Fig. 1b), a large-scale westerly atmospheric circulation with limited vertical air-mass displacement prevailed. In this case (see also Schiemann et al., 2009), the large-scale circulation is steered by the Subtropical Jet Stream (SJS) and embedded synoptic disturbances travelling eastward towards the Himalayas. In contrast, during the monsoon season a southern circulation prevailed with a vertical uplift of air-masses from the Indian sub-continent and Indian Ocean (Fig. 1a), with a clear impact from the low pressure area over the Bay of Bengal (Fig. 1a).

Despite these large-scale circulation features, the local atmospheric circulation at PIL is also characterized by the systematic occurrence of mountain/valley breeze circulation, and prevalent wind directions (SW and NE) are determined by the valley topography. Moreover, a clear link between intra-seasonal precipitation variation and large-scale circulation modes was found by analyzing meteorological parameters at PIL (see Bonasoni et al., 2010). This is evident by inspecting the typical seasonal diurnal variations of wind speed and direction for the period 2012–2014 (Fig. 2). For post-monsoon, winter and pre-monsoon, southerly (valley) winds were evident during the central part of the day, while northerly (mountain) winds occurred during night-time. Typically, night-time winds showed lower speeds compared to the day-time regime. During the monsoon season, southerly winds (from SW to ESE) dominated both day-time and night-time due to the impact of the large-scale monsoon flow between the Indian plains and Tibetan Plateau (Fig. 1a).

The annual mean temperatures measured at PIL (Fig. 3(A)) were −2.9 °C and −2.2 °C in 2012 and 2013, respectively. These values match the annual mean temperature (−2.4 °C) reported by Salerno et al. (2015) for a pluriannual period (1994–2013). For 2014, data was only collected through May, thus annual means are not available. During the study period, the average monthly temperature ranged from −11.9 °C, in January 2012, to 3.7 °C, in July 2013.

The influence of the South Asia monsoon climate results in the highest rainfall between June and September, with the maximum amounts during the study period of 141 and 131 mm in July 2012 and 2013, respectively (Fig. 3(B)). Including snow precipitation in 2013 (42 mm, 11% of total precipitation) and 2014 (65 mm, 17% of total precipitation), the total annual precipitation for 2013 and 2014 was 379 mm and 433 mm, respectively. These totals are lower than the mean total annual precipitation (449 mm y^{-1}) that was measured from 1994 to 2013. Furthermore, Salerno et al. (2015) have indicated that precipitation significantly decreased in the study area during the period 1994–2013, similar to the general trends that are reported for the Himalayan region (Palazzi et al., 2013; Yao et al., 2012).

3.2. Chemical and isotopic composition of precipitation

Precipitation volume-weighted mean (VWM) annual concentrations of the principal ions in wet depositions are given in Table 1. The weighted mean pH measured in the liquid precipitation was near the global mean of 5.7 for pollution-free areas. The main anion was HCO$_3^-$ (Fig. 4) with a concentration 3–5 folds greater than the second major anion NO$_3^-$, while SO$_4^{2-}$ concentrations had the lowest anion values. NH$_4^+$ constituted about 57% of the cations, followed by
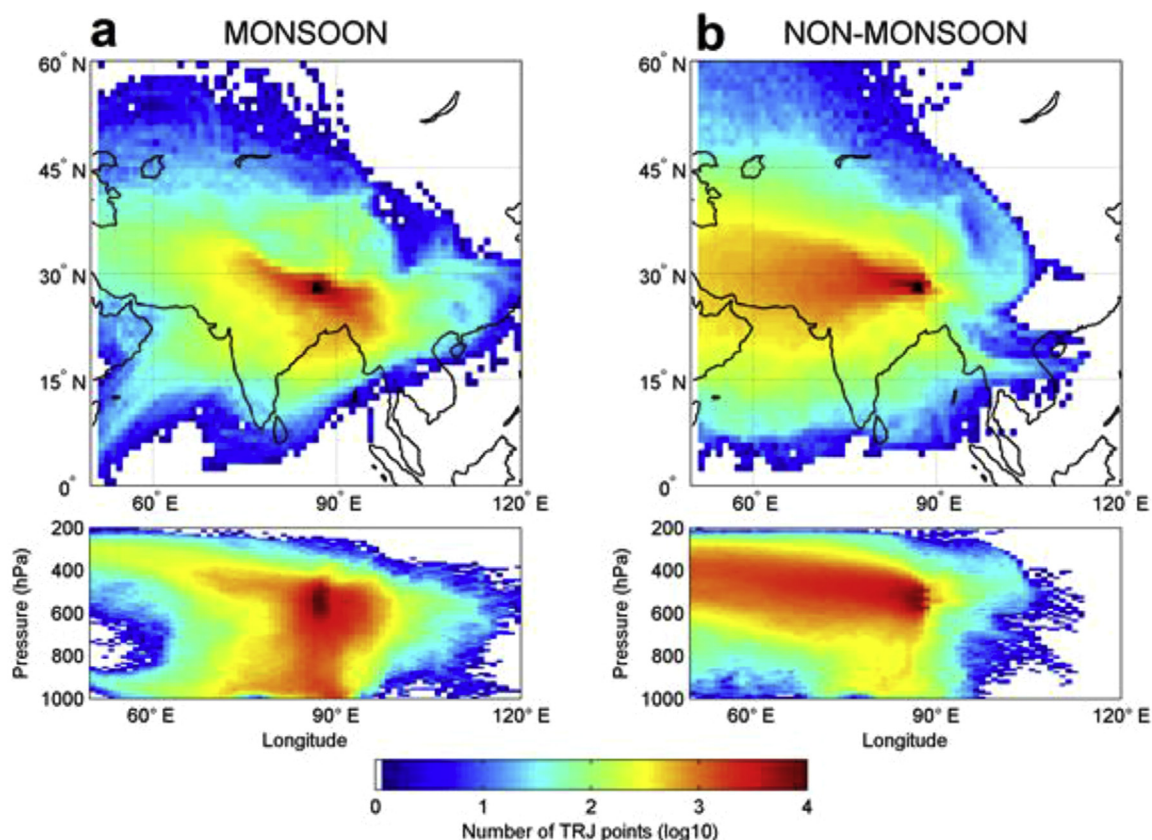
Fig. 1. Concentration field for back-trajectories starting at Nepal Climate Observatory-Pyramid (NCO-P), for the monsoon season (panel a) and during the other seasons (panel b) over the period 2012–2014. For each subplot, the upper panel represents the spatial aggregation of back-trajectory points over a $1° \times 1°$ grid, while the bottom panel indicates the vertical displacement (steps of 10 hPa) as a function of longitude.
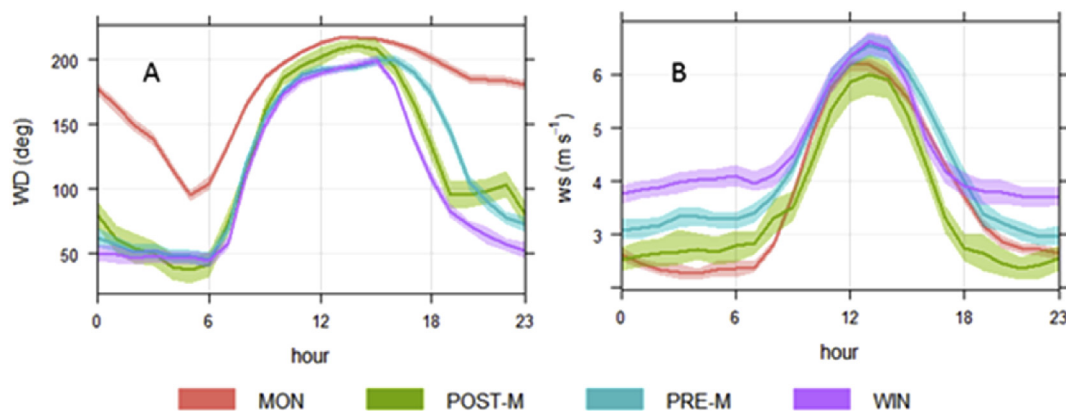
Fig. 2. Seasonally averaged diurnal variations of wind direction (A) and wind speed (B) at Pyramid International Laboratory (PIL). Seasons are defined according to the definition proposed by Bonasoni et al. (2010). The shaded areas represent the 95% confidence intervals.

Ca^{2+} (26.2%), Na^+ (11%), K^+ (3.0%) and Mg^{2+} (2.4%). The concentration of reduced N was greater than the oxidized N form. The chemical composition of precipitation shows distinct differences between rain and snow (Fig. 4). Snow samples were enriched in all analyzed chemical species compared to rain in both years. The greater differences were detected in 2013 when SO_4^{2-} was 13 fold higher, and NO_3^- and NH_4^+ were 5 fold higher than their concentrations in monsoon rain.

A statistical summary of the isotopic compositions recorded during the monsoon and non-monsoon periods is reported in Table 1. Monsoon periods were characterized by a wide range of values (more than 17‰ in $\delta^{18}O$ for 2013), but VWMs of the two years are fully comparable, despite the lack of the first weeks of the period for 2012. Also, these values are in good agreement with those recorded for 2008 (Balestrini et al., 2014). In contrast, enriched values characterize the non-monsoon period, which also corresponds to low amounts of precipitation, primarily occurring as snow.

The isotopic compositions of precipitation (both rain and snow) are shown on the classical δ^2H vs $\delta^{18}O$ diagram in Fig. 7,
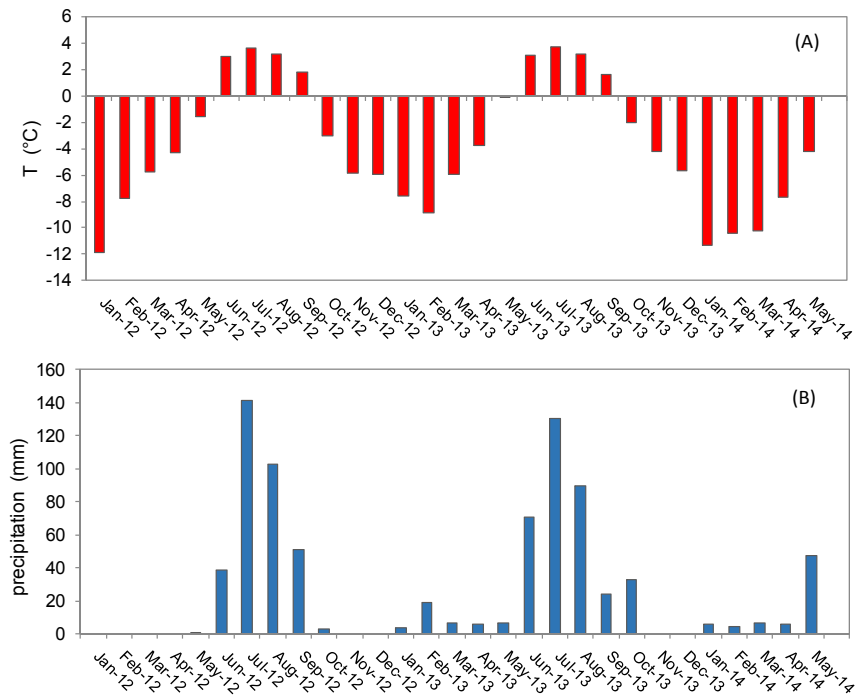
Fig. 3. Monthly averaged diurnal variations of temperature (A) and amount of precipitation (B) at Pyramid International Laboratory (PIL).

distinguished based on their seasonality. All samples fall close to the Global Meteoric Water Line (GMWL) reported by Rozanski et al. (1993), except for one sample corresponding to a very low amount of precipitation, which could have suffered from preservation problems (i.e., evaporation) and is therefore considered an outlier.

The regression line for all precipitation data follows the equation:

$$\delta^2 H = 8.17 \,(\pm 0.13)\, \delta^{18}O + 16.6 \,(\pm 2.3)\, (R^2 = 0.993; \, n = 31; \, p < 0.01)$$

This regression compares well with that calculated for monsoon precipitation collected at the same location in 2008, and with

others from similar regions (Balestrini et al., 2014 and references therein).

The observed outcomes confirm previous results (Balestrini et al., 2014) indicating that the ion concentrations in the rainfall at PIL were the lowest among the concentrations measured at high elevation sites around the world (Li et al., 2007; Liu et al., 2015; Tripathee et al., 2014; Williams et al., 2009). Comparable concentrations of most ionic species were recorded in fresh snow samples collected in the Central Himalaya at different altitudes, ranging from 5700 to 6400 m a.s.l. (Balerna et al., 2003). These findings suggest that the chemical concentrations measured at PIL can be considered the regional background concentrations in wet

Table 1
Concentrations (as volume weighted mean) of the main ionic species and stable isotopes of the water molecule recorded during the monsoon and non-monsoon periods. Isotopic data for 2014 non-monsoon season not included because isotopic results not available.

|	pH	NO_3^-	SO_4^{2-}	Cl^-	HCO_3^-	NH_4^+	Na^+	K^+	Mg^{2+}	Ca^{2+}	$\delta^{18}O‰$	$\delta^2H‰$	d-excess
						$\mu eq\ l^{-1}$							
Monsoon 2012													
N	8	12	12	12	12	12	12	12	12	12	10	10	10
VWM	5.93	2.01	0.84	1.74	9.81	9.75	1.66	0.31	0.12	2.51	−17.74	−129.4	12.6
Min	5.58	1.06	0.50	0.90	0.00	2.27	0.36	0.08	<D.L	1.32	−24.28	−180.2	11.3
Max	6.37	14.43	4.79	5.63	23.84	23.34	3.48	0.83	1.23	17.97	−14.92	−108.0	14.4
Monsoon 2013													
N	15	15	15	15	15	15	15	15	15	15	12	12	12
VWM	6.01	2.13	0.99	1.89	7.20	4.76	1.05	0.39	0.40	3.53	−17.81	−131.2	11.8
Min	5.25	0.66	0.25	0.65	2.00	0.14	0.26	0.05	0.19	0.81	−24.47	−181.1	6.5
Max	6.23	21.70	8.14	8.83	36.74	33.27	5.70	3.15	2.47	30.24	−6.71	−39.9	15.8
Snow 2013													
N	8	12	12	12	11	12	12	12	12	12	12	12	12
VWM	5.53	11.03	13.04	6.35	14.03	22.09	3.34	3.50	1.99	15.60	−17.81	−131.2	11.8
Min	5.24	2.17	1.83	2.78	0.75	11.28	0.87	0.29	0.41	4.09	−24.47	−181.1	6.5
Max	6.60	111.2	104.7	37.65	120.5	159.2	20.44	22.23	20.72	158.03	−6.71	−39.9	15.8
Snow 2014													
N	8	10	10	10	10	9	10	10	10	10			
VWM	5.82	4.33	5.43	2.10	8.81	4.91	2.12	0.98	1.95	10.47			
Min	5.46	0.71	0.57	0.94	1.00	2.18	0.83	0.28	0.62	1.75			
Max	6.16	30.70	27.73	17.23	120.4	61.25	30.70	5.91	9.21	49.75			
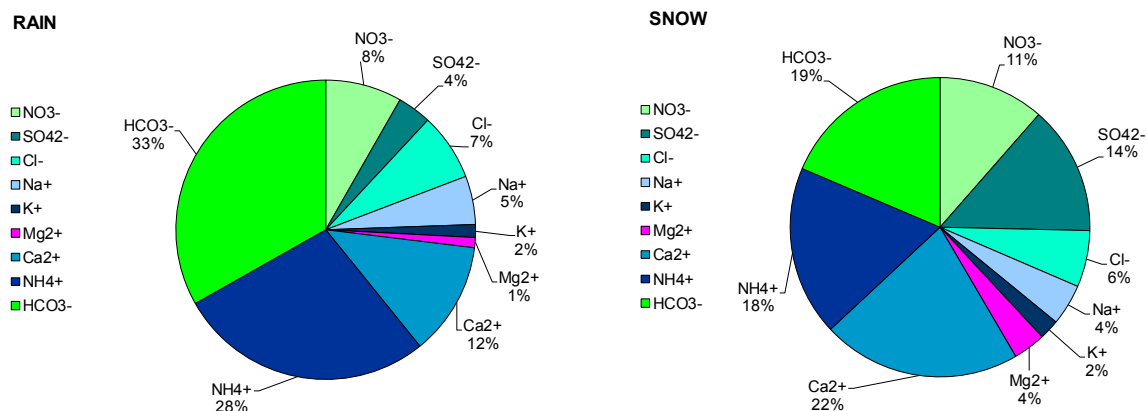
Fig. 4. Average chemical composition of rain and snow collected during the study period. Data were derived using the average concentrations of samples weighted for the amount of rainfall/snow.

deposition. One reason that could explain the higher concentrations of most ions measured in snow deposition relative to rain could be the higher efficiency of snow to scavenge aerosols particles (Wang et al., 2014 and references therein). Since we collected fresh snowfall events, not snowpack, dry deposition did not contribute to enrichment of our snow samples. In order to evaluate further explanations for the described differences, it is necessary to define the origin of the chemical species.

3.3. Ion sources

The relationships between chemical species in monsoon rainfall provide insight into the principal precursors of ions in summer wet deposition. We found a significant linear regression between Na^+ and Cl^- ($R^2 = 0.524$; $p = 1.95E-05$) with a slope (1.20) that is very near the classical sea-salt ratio, 1.17 (Keene et al., 1986), indicating the presence of marine aerosols (Fig. 5(a)). Ca^{2+} and Mg^{2+} were also significantly correlated ($R^2 = 0.606$; $p = 1.77E-06$) (Fig. 5(b)), suggesting a contribution from geochemical weathering of rock and soil. The strong significant linear regression between NO_3^- and SO_4^{2-} ($R^2 = 0.880$; $p = 3.12E-13$) suggests common precursors, i.e., SO_2 and NO_x emitted from anthropogenic sources such as fossil fuels (Fig. 5(c)).

In general, we found similar relationships in snow samples, suggesting that the ions described above originated from the same sources in the non-monsoon season as well. However, a notable difference was observed for NH_4^+ in snow (Fig. 6), where it was linearly correlated with SO_4^{2-} and NO_3^- ($R^2 = 0.794$, $p = 3.64E-08$ and $R^2 = 0.606$, $p = 1.94E-05$, respectively). These relationships, even if statistically significant ($p = 0.02$ and 0.009, for SO_4^{2-} and NO_3^-, respectively) explained a smaller fraction of NH_4^+ variability in rainfall samples (20.6 and 24.2%) than in snow samples (79.4 and 60.6%). Ammonium sulfate and nitrate aerosols are formed by a gas-phase reaction of ammonia with sulfuric and nitric acids, which are generated by the oxidation of compounds such as sulfur dioxide and nitrogen oxides (Dentener and Crutzen, 1994; Wayne, 1991). The NH_4^+/SO_4^{2-} and NH_4^+/NO_3^- ratios in rainfall had mean values of 6.0 and 3.0, which indicated that a fraction of NH_4^+ was not neutralized by SO_4^{2-} and NO_3^- but most likely by HCO_3^- (Fig. 5(d)). The conversion of NH_3 to the NH_4^+ aerosol depends on the concentrations of strong acids in the atmosphere (Walker et al., 2000), which were likely very low at the PIL during the monsoon time. The fraction of ammonium associated with sulfate and nitrate likely originated from anthropogenic sources while the other fraction could be related to natural sources, primarily from cultivated lands

and vegetated soils as well as from animal excreta and biomass burnings. The significant positive linear relationship between K^+ and NH_4^+ ($R^2 = 0.41$, $p = 0.0002$) could be interpreted as a signal of biomass burning, a common practice in the rural villages of Nepal (Shrestha et al., 2002). In snow samples the NH_4^+/SO_4^{2-} and NH_4^+/NO_3^- ratios decreased to 2.5 and 1.5 suggesting an increased contribution from anthropogenic emissions and a simultaneous decrease in NH_3 soil emissions during the winter.

3.4. Seasonal variations: atmospheric circulation and precipitation amount effect

The sampling of snow precipitation during 2013 and 2014 allowed us to obtain a complete wet deposition data set including all seasons (monsoon, post-monsoon, winter and pre-monsoon), thereby characterizing the Khumbu weather regime. Even so, given the few snow events and the shortness of some seasons (post-monsoon and winter) we analyzed the difference between samples grouped into monsoon and non-monsoon seasons. For all analyzed species, except HCO_3^-, we found high statistical significance in the differences ($p < 0.01$) between the two groups, with higher concentrations in the non-monsoon period. Particularly during 2013, elevated concentrations of NO_3^-, SO_4^{2-} and NH_4^+ were measured in the first winter snow event, and in May at the end of the pre-monsoon season.

The detection of combustion emission "fingerprints" in these snow samplings, reflects similar features in the atmospheric composition from other observations carried out in the same region. Indeed, during winter and especially the pre-monsoon season, "acute pollution events' characterized by high O_3, BC, and PM_{1-10} (i.e. atmospheric particulate mass) were identified by Marinoni et al. (2010, 2013) at the PIL area and were even detected inside the Tibetan Plateau (Zhao et al., 2013). The present additional findings from snow chemistry testify to the transport of pollution from anthropogenic emissions and open vegetation fires from the Himalayan foothills and Indian sub-continent up to the Himalaya region. Moreover, "acute" pollution events related to air-mass transport from the planetary boundary layer (PBL) of the Indo-Gangetic plains were systematically identified by Cristofanelli et al. (2014) during the summer monsoon onset period (i.e. from May to June).

Our results are consistent with those reported by Shrestha et al. (2002) who observed 25 and 18 fold higher NH_4^+ and SO_4^{2-} concentrations, respectively, in the pre-monsoon than in the monsoon season at a lower site in the Khumbu Valley. Fresh snow collected
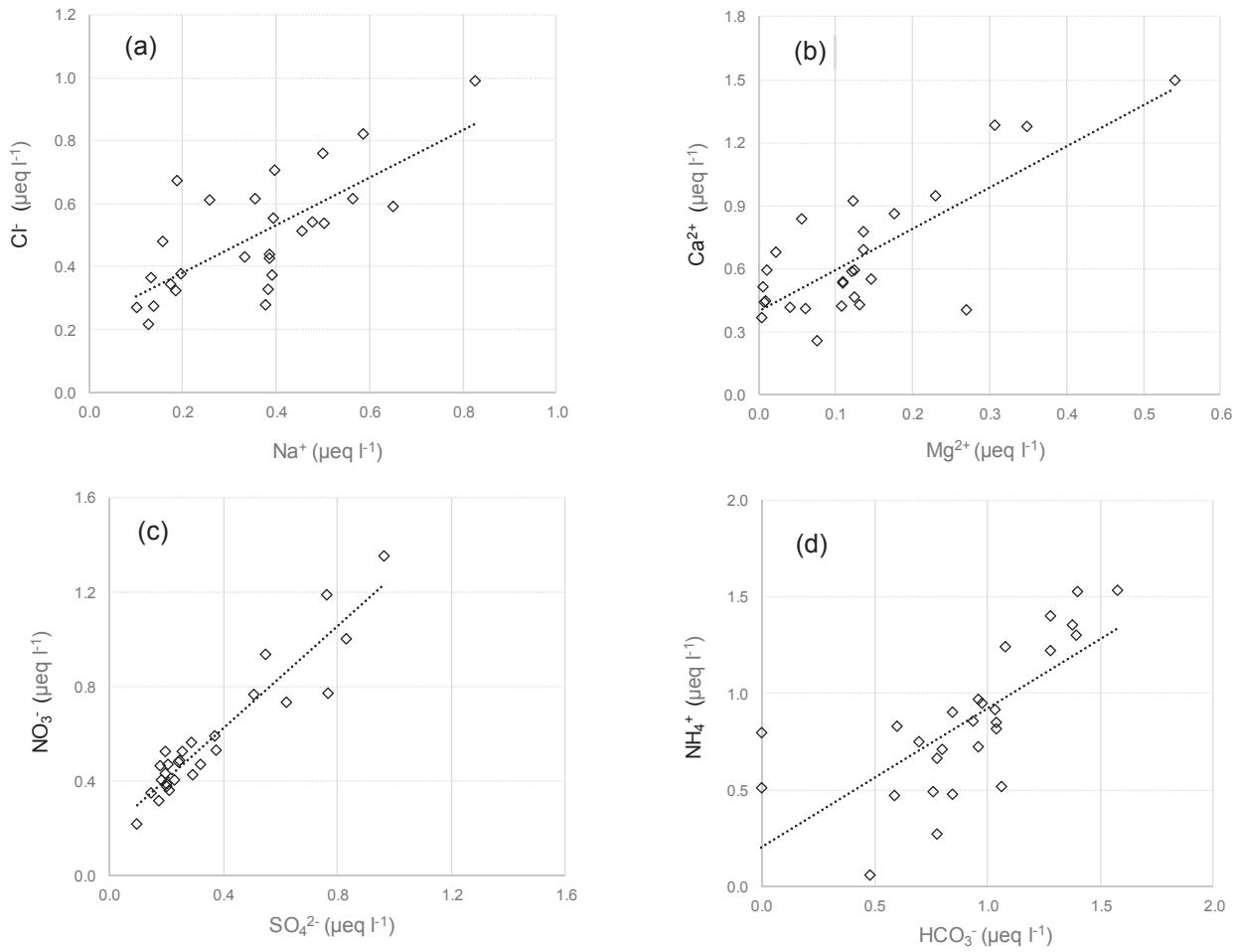
Fig. 5. Linear regression between the log-transformed concentrations of Cl^- vs Na^+ (a), Ca^{2+} vs Mg^{2+} (b), NO_3^- vs SO_4^- (c) and NH_4 vs HCO_3^- in weekly rainfall samples.
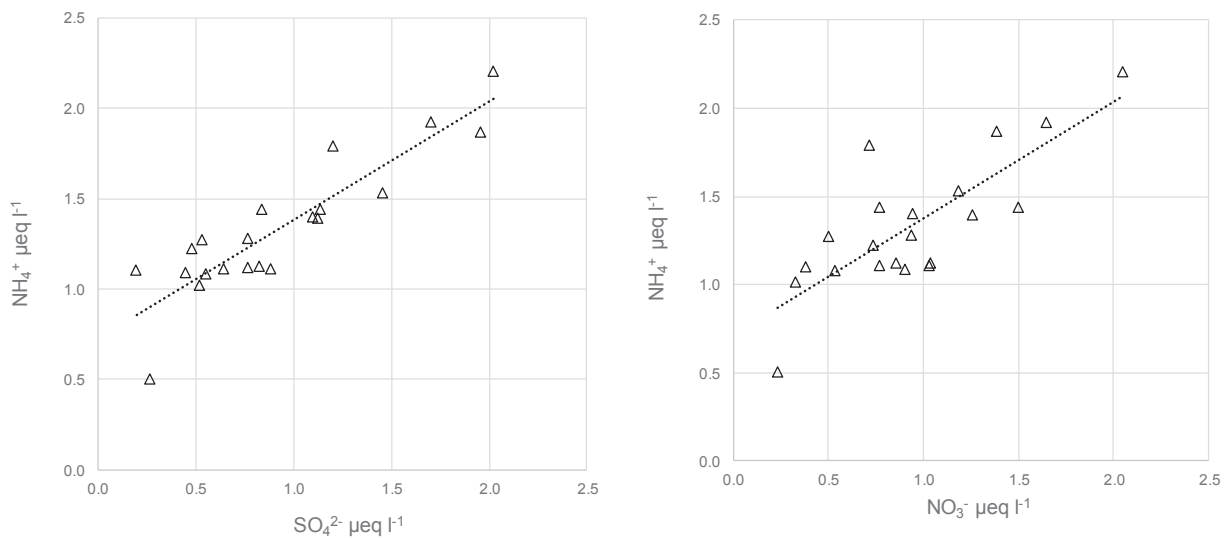
Fig. 6. Linear regression of NO_3^- with NH_4^+ (left) and SO_4^{2-} with NH_4^+ (right) log-transformed concentrations in snow precipitation during winter seasons 2013 and 2014.

on the northern and southern slope of the Himalayan ranges shows differences between the monsoon season, when values are not substantially influenced by anthropogenic inputs, and the non-monsoon (post-monsoon, winter and pre-monsoon) season

which is characterized by the influence of dust from Central Asia (Balerna et al., 2003; Jenkins et al., 1987; Marinoni et al., 2001; Kang et al., 2002). Higher concentrations of most chemical species in non-monsoon compared with monsoon deposition have also been observed along an altitude gradient (1314–4417 m a.s.l.) on the southern slope of the Central Himalayas (Nepal) (Tripathee et al., 2014). At Nam Co station, on the Western Tibetan Plateau the highest concentration of crustal ions in precipitation occurred from February to April; in contrast, NH_4^+ and NO_3^- exhibited high concentrations from May to August due to enhanced local grazing activities close to the monitoring area (Li et al., 2007).

Analogously to 2008 (Balestrini et al., 2014), during 2012 and 2013 some chemical species exhibited a pattern within the monsoon period partially connected with the precipitation amount. As shown in Fig. 8(a), SO_4^{2-} and NO_3^- concentrations reached a maximum at the beginning of the monsoon, then decreased with increasing precipitation volume during the monsoon. By September, the concentrations increased again as precipitation volume decreased. The NH_4^+ concentrations exhibited a similar pattern, but showed elevated values in July as well (Fig. 8(b)). Similar SO_4^{2-} and NO_3^- temporal behavior has been recorded at other sites located in the same climatic zone (Shrestha et al., 2002). A dilution effect was expected during the monsoon rainfall and was supported by the significant inverse power relationships between the NO_3^- and SO_4^{2-} concentrations and the precipitation amounts ($R^2 = 0.833$, $p < 0.001$ and $R^2 = 0.745$, $p < 0.001$, respectively) as shown in Fig. 9. This relationship can be explained by the scavenging of aerosols during the first phase of the monsoon season and a more gradual effect of rainout during the following period. In the case of NH_4^+, the relationship with amount of rainfall was not significant, likely because an additional factor – natural emissions of NH_3 during the warmer days – influenced the NH_4^+ concentration of the rain.

In line with these findings, the results obtained from the aerosol monitoring at NCO-P (5079 m a.s.l.), revealed minimum concentrations of carbonaceous and ionic aerosols during the monsoon season (Fig. 1 in Decesari et al., 2010, Fig. 2 in Marinoni et al., 2010). The observation of enrichment of NH_4^+ during July, similar to Shrestha et al. (2002) for a site at an altitude of 4100 m a.s.l. in the Khumbu, likely resulted from the scavenging of gaseous NH_3, which is emitted by cultivated lands, vegetated soils and livestock in the low-lying valley and transported to the PIL by ascending air masses.

Further constraints on the origin of ions in precipitation are provided by isotopic data, which can be used to trace the origin of the water vapor masses in support of the computed back-trajectories. During the monsoon period a progressive isotopic depletion was observed, with the more depleted values recorded in August, also corresponding to intense precipitation (Fig. 10). This trend is common in precipitation that originates from the Indian summer monsoon, and is attributed by some authors (e.g. Kumar et al., 2010) to the so-called "amount effect" (Rozanski et al., 1993). Indeed, a significant inverse correlation with the amount of precipitation existed ($R^2 = 0.163$; n = 49; $p < 0.01$ for $\delta^{18}O$) at our study site, although it may be argued that this correlation is affected by the combined use of weekly and daily precipitation values. In contrast, during the non-monsoon period, an isotopic enrichment trend was observed (Fig. 10), with more enriched values recorded in March. Also in this case, a significant inverse correlation existed with the precipitation amount ($R^2 = 0.532$; n = 8; $p < 0.05$ for $\delta^{18}O$), although not as strong as the one observed for the monsoon period. Since some chemical species also exhibited a trend during the monsoon, partially connected with the precipitation amount, we could conclude that the temporal evolution of the ionic contents during the monsoon is determined by the same factors as that of the isotopic compositions, i.e. the amount of
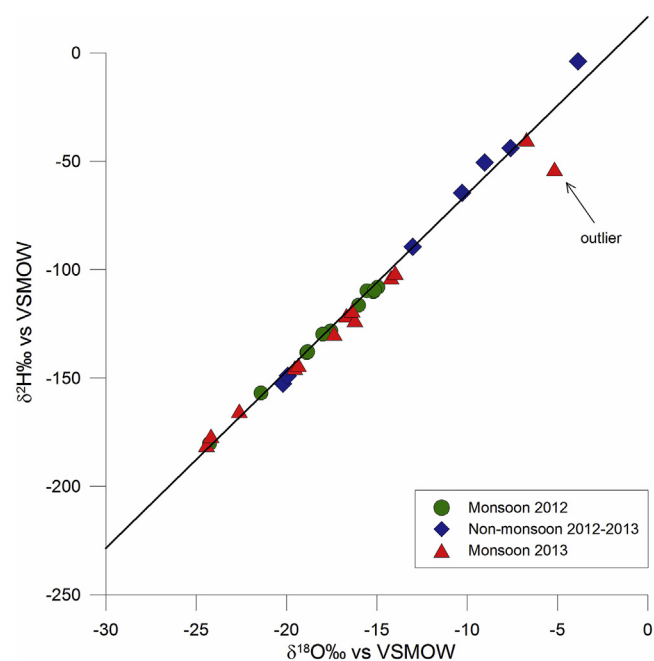

Fig. 7. Stable isotope composition of precipitation samples distinguished based on seasonality. The regression line based on all data follows the equation $\delta^2H = 8.17$ (±0.13) $\delta^{18}O + 16.6$ (±2.3).

precipitation. Nevertheless, when trying to relate the ionic contents with the isotopic composition, no significant correlation appears, confirming that other factors should be taken into account, namely the origin of the water vapor masses.

The d-excess has been widely used as a diagnostic tool to measure the contribution of water vapor from different sources at a given location (Clark and Fritz, 1997; Jeelani et al., 2013). More specifically, low values should correspond to moisture supplied from the Indian Ocean and the Bay of Bengal, while high values should correspond to continental moisture carried by the western disturbances (Breitenbach et al., 2010; Jeelani et al., 2013).

High (>15‰) and low (<10‰) d-excess values were observed in both the monsoon and the non-monsoon periods (Table 1). During the monsoon, the d-excess values increased with the decrease of the isotopic compositions (Fig. 10), with a significant negative correlation ($R^2 = 0.279$; n = 49; $p < 0.01$ for $\delta^{18}O$). Two moisture source areas, the Indian Ocean and the Bay of Bengal, characterize the different stages of the Indian monsoon (e.g., Breitenbach et al., 2010; Gupta and Deshpande, 2003; Sengupta and Sarkar, 2006), and a change between these sources could account for the enriched isotopic compositions and the associated high ionic contents found at the beginning and end of the season. However, at our study site this change cannot be clearly evidenced, as it is overprinted by the "amount effect" (Balestrini et al., 2014). By contrast, during the non-monsoon period the increase in the d-excess values was positively correlated to the isotopic compositions ($R^2 = 0.877$; n = 8; $p < 0.01$ for $\delta^{18}O$). Since the isotopic compositions were strongly correlated to the precipitation amount, this would indicate that during the monsoon period, precipitation occurred from water vapor originated from the Indian Ocean and the Bay of Bengal, while, during the non-monsoon period, precipitation occurred from water vapor of more continental origin: in the latter case, both enriched isotope values and higher NO_3^- and SO_4^{2-} concentrations could be ascribed to the change in air circulation patterns.
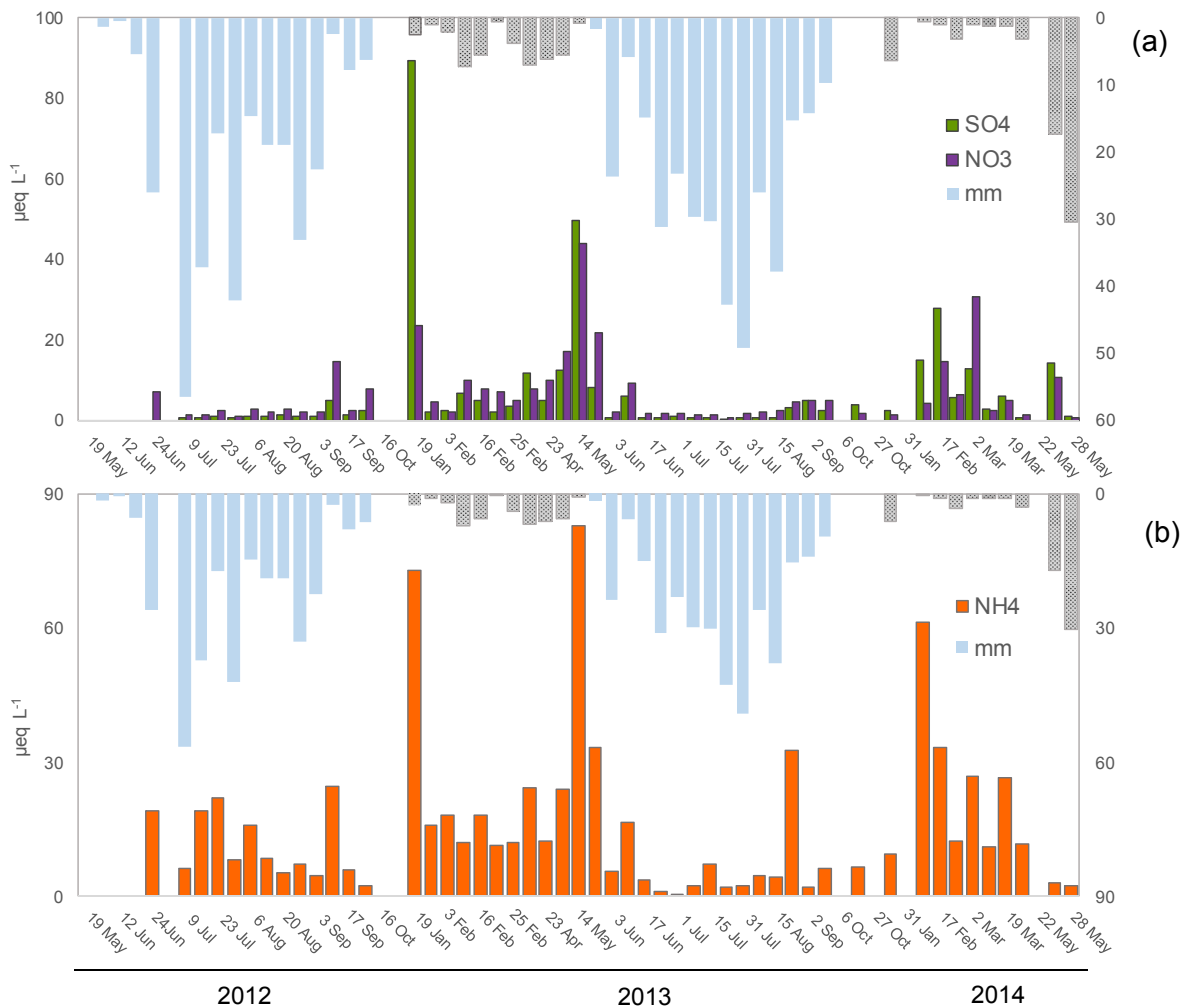
Fig. 8. Timeline of NO_3^- and SO_4^{2-} (a) and NH_4^+ (b) concentrations with precipitation volume.
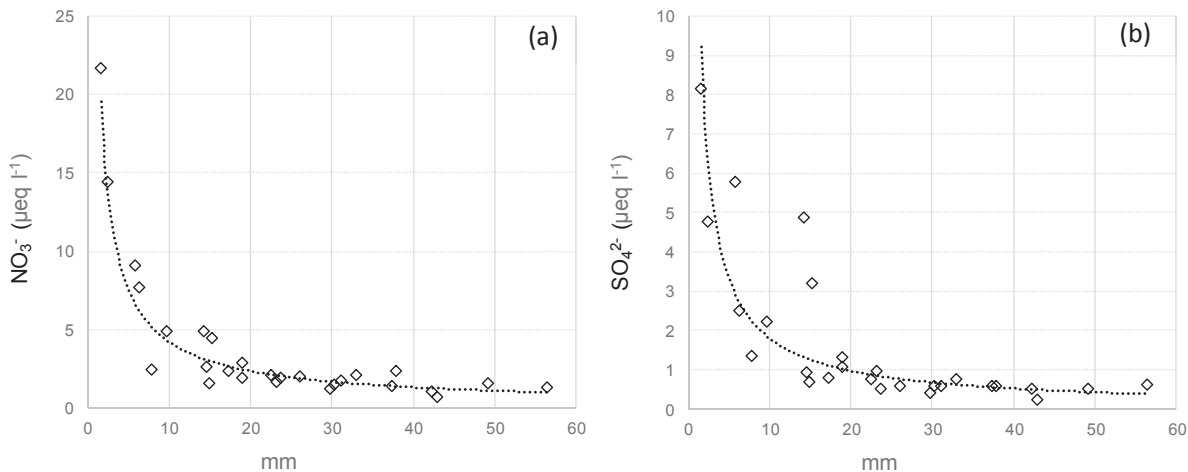

Fig. 9. Relationship between nitrate (a) and sulfate (b) with the amount of rainfall (mm). The best-fit line is indicated in each graph.

3.5. Temporal comparison

The comparison between VWM concentrations measured in monsoon precipitation collected in the periods 1991 and 1992 (Valsecchi et al., 1999), 2008 (Balestrini et al., 2014), and 2012 and 2013 (present data) provides indications about potential changes over time. Despite significant industrial growth in India and China in the last decades, the present VWM concentrations of NO_3^- and
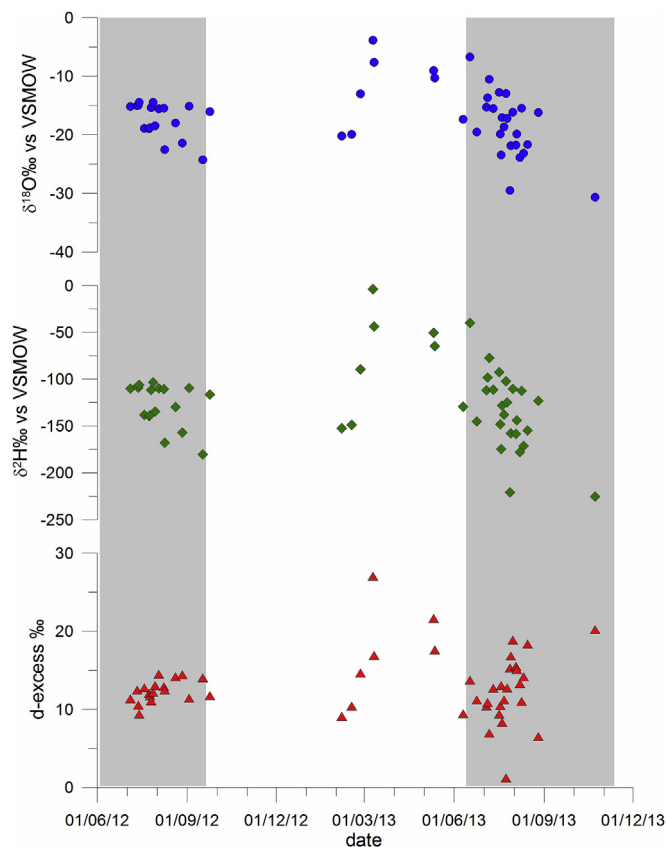
Fig. 10. Temporal trends of the isotopic composition and of the d-excess in precipitation. The grey areas represent the monsoon seasons.

SO_4^{2-}, which are fossil fuel combustion tracers, do not statistically differ from those that were measured in the early 1990s (Fig. 11). This finding suggests that the tropospheric background concentrations may not have changed significantly in the Himalayas from the early 1990s to the present. The previously observed reduction of ions of marine origin (Na^+, Cl^- and K^+) (Balestrini et al., 2014) has not been confirmed by the addition of 2012 and 2013 data. The only chemical species that seems to increase from the 1990s is NH_4^+ whose VWM concentration rises from 1 µeq l^{-1} to 9.8 and 4.8 µeq l^{-1} in 2012 and 2013, respectively. This result could be partially explained by the use of a bactericide added to the samples from 2012 that avoids the loss of non-conservative ions. Thus, one hypothesis is that the NH_4^+ concentrations measured in 1990−1991 and 2008 were likely underestimated. Nonetheless we cannot exclude the possibility of an effective increase of wet-deposited NH_4^+ especially in light of an NH_4^+ record covering the period 1845−1997, reconstructed using a Mount Everest ice core (Kang et al., 2002). That study reported a dramatic NH_4^+ increase since the 1950s that was in part explained by an increase in temperature that caused the strengthening of natural ammonia emissions (e.g., from plants and soils).

3.6. Wet deposition fluxes and comparison with remote ecosystems

Annual SO_4^{2-} and inorganic N (N_{in} = sum of NH_4^+ and NO_3^-) deposition fluxes at the high Khumbu Valley were 0.47 and 0.56 kg ha^{-1} y^{-1} respectively, for the complete year of 2013 (Table 2). In general, for all analyzed species the contribution of the snow component to the total deposition was substantial, despite the differences in the precipitation volumes. The contributions of

snow-deposited SO_4^{2-} and inorganic N were 54% and 34% of the total annual flux (snow plus rainfall), respectively. In 2013, we observed a prevalence of NH_4^+ (69% of N_{in}) relative to NO_3^- (31%) in the wet deposition flux (rainfall plus snow). A similar N pattern was reported for the Tibetan Plateau and likely reflects a global tendency emerging from recent measurements and model-based results (Vet et al., 2014) that indicate $N_{reduced}$ as the dominant contributor to N wet deposition (i.e., ratios> 60%) in India and East Asia.

Comparing the results of this work with results available from
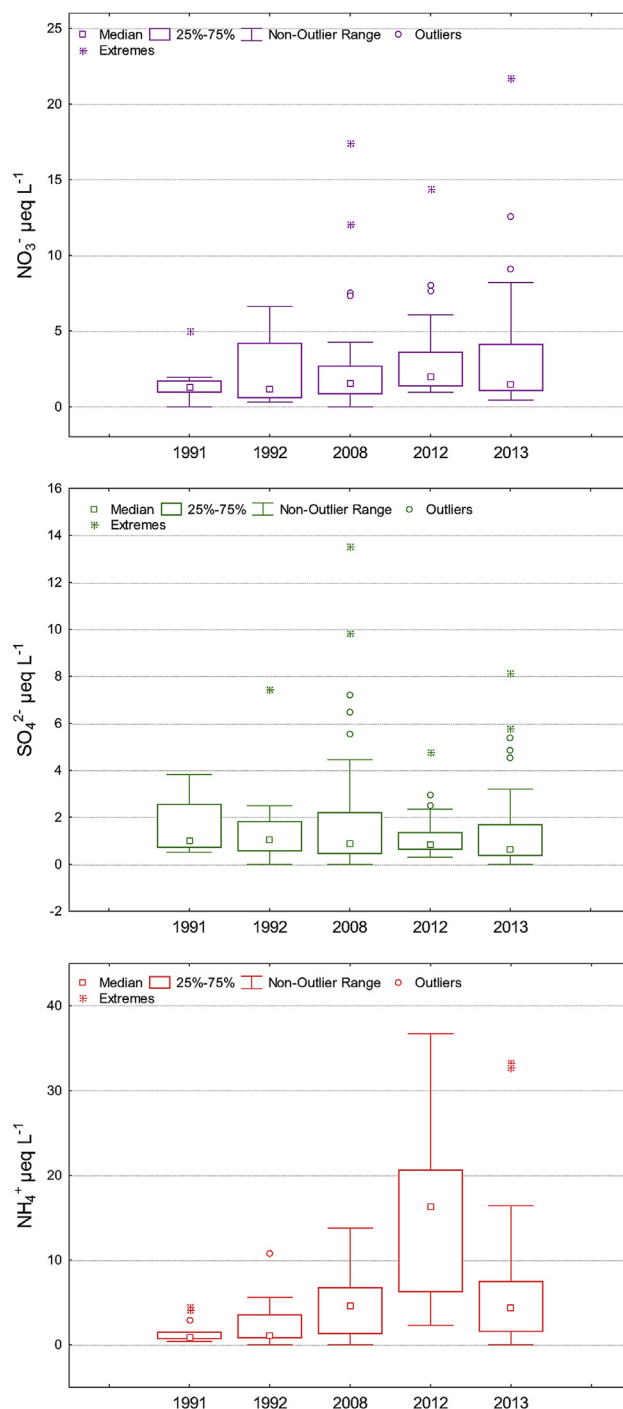
Fig. 11. Annual VWM concentrations of nitrate, sulfate, and ammonia measured at Pyramid International Laboratory (PIL).

Table 2
Fluxes (kg ha^{-1} y^{-1}) of the main chemical species of monsoon precipitation and snow collected at the Pyramid from July 2012 to May 2014. The amounts of rain and snowfall (mm) are shown.

	mm	N$_{in}$	N-NO$_3^-$	SO$_4^{2-}$	Cl$^-$	N-NH$_4^+$	Na$^+$	K$^+$	Mg^{2+}	Ca^{2+}
Monsoon 2012	278	0.46	0.08	0.11	0.17	0.38	0.11	0.03	0.004	0.14
Monsoon 2013	355	0.34	0.11	0.17	0.24	0.24	0.04	0.14	0.03	0.20
Snow 2013	42	0.20	0.07	0.26	0.09	0.13	0.03	0.03	0.01	0.13
Snow 2014	65	0.08	0.04	0.17	0.05	0.04	0.03	0.02	0.02	0.14

other Asian sites indicates that N$_{in}$ wet deposition fluxes of the same order of magnitude (0.50 - 0.90 kg ha^{-1} y^{-1}) occur on the eastern Tibetan Plateau, while higher values have been measured on the western side (1.5–3.1 kg ha^{-1} y^{-1}) (Liu et al., 2015). SO$_4^{2-}$ fluxes ranging between 1.1 and 4.5 kg ha^{-1} y^{-1} were reported for some of these sites (Liu et al., 2013). The N$_{in}$ and SO$_4^{2-}$ fluxes measured at PIL were an order of magnitude lower than those measured in the Rocky Mountains (2.0 and 10.0 kg ha^{-1} y^{-1}, respectively) (Benedict et al., 2013; Heath and Baron, 2014) and two orders of magnitude lower when compared with those measured in the Italian Alps (6–15 kg ha^{-1} y^{-1} and 5–14 kg ha^{-1} y^{-1}, respectively) (Marchetto et al., 2014).

Given the importance of N cycling from an ecological point of view, we extended this comparison to other ecosystems in the most remote regions of the world. We found that atmospheric nitrogen loads were only similar for the Khumbu valley and the Hawaiian Islands (0.60 kg ha^{-1} y^{-1}) (Heath and Huebert, 1999). N loads that were 6–10 fold higher were reported for Northern Africa dry savanna (Galy-Lacaux et al., 2009) and the Central Amazonia tropical rain forest (Pauliquevis et al., 2012). The estimated annual N deposition can be understood in the context of critical loads, thresholds for significant harmful effect on natural resources developed in the 1990's as a basis for negotiating control strategies for air pollution (Posch et al., 1997). Recently, the critical load of N wet deposition has been proposed at <1.5 ± 1 kg N ha^{-1} y^{-1} for aquatic ecosystems in high elevation basins with steep slopes, sparse vegetation, and an abundance of exposed bedrock and talus, such as those of the US Rocky Mountains (Nanus et al., 2012). As that value is threefold the N load measured at PIL, it seems unlikely that current levels of N deposition should have discernible ecological effects related to N saturation. However, the NO$_3^-$ concentrations measured in surface waters of the high Khumbu catchment were relatively higher than the theoretically expected values based on the extremely low N input from wet deposition (Balestrini et al., 2014). We must take into account that contribution of dry deposition in the Himalayan region, where dry conditions occur for 8–9 months in a year, could be significant. Nevertheless, problems associated with measuring and modeling dry deposition flux limit the availability of estimates of its contribution to total deposition, particularly at remote sites (Fowler et al., 2009). In the literature, 25–30% of the total inorganic N deposition occurs by dry deposition in the Rocky Mountains in Colorado and southern Wyoming (Burns, 2003) and Balestrini et al. (2000) reported a NO$_3^-$ dry deposition contribution of approximately 25% for Italian alpine sites located at an elevation of 1100 m a.s.l. This suggests that total N deposition to our study area could be underestimated by at least 25%.

4. Conclusions

The long-term monitoring of wet deposition chemistry at high elevation in the Himalayan region acquires a particular relevance in light of the recent recommendation of WMO-GAW Scientific Advisory Group for Precipitation Chemistry (SAG-PC) to increase atmospheric deposition monitoring in regions of strong population growth and industrial development, areas of high ecosystem sensitivity and intensifying agricultural activity, and regions where biomass burning is common. The Himalayan region matches most of these requisites lying between India and China, being very sensitive to global changes and hosting rural population who historically burn biomass.

The chemistry of the precipitation during monsoon conditions indicates that depositions at high-elevation sites at this time are not substantially influenced by anthropogenic inputs because the air masses reaching the PIL during the monsoon season are nearly depleted of potential contaminants that originate from the lower urbanized Indian areas, and are likely deposited at lower altitudes. The comparison of our results with previous measurements collected in the early 1990's shows no statistically significant differences between the two periods, suggesting that there may not be an increasing level of contaminants in the monsoon rainfall, despite increasing atmospheric pollution emissions in India and China. However, the Himalayas are not an effective barrier against pollutants coming from long range transport, as evidenced during the pre-monsoon season and in the summer monsoon onset period when the concentrations of combustion emission tracers increased.

The contribution of snow to wet deposition fluxes was significant for all analyzed species, but especially for sulfate, despite the smaller volume relative to rain. The annual estimated wet N deposition was lower than the critical load of N for high elevation ecosystems. However, the recent published data on nitrate concentration in the surface waters of the study area are relatively elevated. The findings of this study further emphasize the need for additional research efforts to deepen the understanding of processes occurring in the dry season and obtaining a complete assessment of the total atmospheric deposition including the dry deposition component.

References

Balerna, A., Bernieri, E., Pecci, M., Polesello, S., Smiraglia, C., Valsecchi, S., 2003. Chemical and radiochemical composition of fresh snow samples from northern slope of Himalayas (Cho Oyu range, Tibet). Atmos. Environ. 37, 1573–1581.

Balestrini, R., Galli, L., Tartari, G., 2000. Wet and dry atmospheric deposition at prealpine and alpine sites in northern Italy. Atmos. Environ. 34, 1455–1470.

Balestrini, R., Polesello, S., Sacchi, E., 2014. Chemistry and isotopic composition of precipitation and surface waters in Khumbu valley (Nepal Himalaya): N dynamics of high elevation basins. Sci. Total Environ. 485, 681–692.

Baudo, R., Schommer, B., Belotti, C., Vuillermoz, E., 2007. From Himalaya to Karakoram: the spreading of the project Ev-K2-CNR. In: Baudo, R., Tartari, G., Vuillermoz, E. (Eds.), Mountains: Witnesses of Global Changes. Research in the Himalaya and Karakoram: Share-asia Project. Elsevier, Amsterdam, pp. 33–50. Developments in Earth Surface Processes, vol. 10.

Benedict, K.B., Carrico, C.M., Kreidenweis, S.M., Schichtel, B., Malm, W.C., Collett Jr., J.L., 2013. A seasonal nitrogen deposition budget for Rocky Mountain National Park. Ecol. Appl. 23 (5), 1156–1169.

Bertolani, L., Bollasina, M., Tartari, G., 2000. Recent biennial variability of meteorological features in the Eastern Highland Himalayas. Geophys. Res. Lett. 27 (15), 2185–2188.

Bonasoni, P., Laj, P., Marinoni, A., Sprenger, M., Angelini, F., Arduini, J., Bonafè, U., Calzolari, F., Colombo, T., Decesari, S., Di Biagio, C., di Sarra, A.G., Evangelisti, F., Duchi, R., Facchini, M.C., Fuzzi, S., Gobbi, G.P., Maione, M., Panday, A., Roccato, F., Sellegri, K., Venzac, H., Verza, G.P., Villani, P., Vuillermoz, E., Cristofanelli, P., 2010. Atmospheric brown clouds in the Himalayas: first two years of continuous observations at the Nepal Climate Observatory-Pyramid (5079 m). Atmos. Chem. Phys. 10, 7515–7531.

Bonasoni, P., Laj, P., Angelini, F., Arduini, J., Bonafè, U., Calzolari, F., Cristofanelli, P., Decesari, S., Facchini, M.C., Fuzzi, S., Gobbi, G.P., Maione, M., Marinoni, A., Petzold, A., Roccato, F., Roger, J.C., Sellegri, K., Sprenger, M., Venzac, H., Verza, G.P., Villani, P., Vuillermoz, E., 2008. The ABC-Pyramid Atmospheric Research Observatory in Himalaya for aerosol, ozone and halocarbon measurements. Sci. Total Environ. 391, 252–261.

Breitenbach, S.F.M., Adkins, J.F., Meyer, H., Marwan, N., Krishna Kumar, K., Haug, G.H., 2010. Strong influence of water vapor source dynamics on stable isotopes in precipitation observed in Southern Meghalaya, NE India. Earth Planet. Sci. Lett. 292, 212–220.

Burns, D.A., 2003. Atmospheric nitrogen deposition in the Rocky Mountains of Colorado and southern Wyoming—a review and new analysis of past study results. Atmos. Environ. 37, 921–932.

Clark, I., Fritz, P., 1997. Environmental Isotopes in Hydrogeology. Lewis Publishers, Boca Raton.

Cristofanelli, P., Putero, D., Adhikary, B., Landi, T.C., Marinoni, A., Duchi, R., Calzolari, F., Laj, P., Stocchi, P., Verza, G., Vuillermoz, E., Kang, S., Ming, J., Bonasoni, P., 2014. Transport of short-lived climate forcers/pollutants (SLCF/P) to the Himalayas during the South Asian summer monsoon onset. Environ. Res. Lett. 9, 084005. http://dx.doi.org/10.1088/1748-9326/9/8/084005.

Decesari, S., Facchini, M.C., Carbone, C., Giulianelli, L., Rinaldi, M., Finessi, E., Fuzzi, S., Marinoni, A., Cristofanelli, P., Duchi, R., Bonasoni, P., Vuillermoz, E., Cozic, J., Jaffrezo, J.L., Laj, P., 2010. Chemical composition of PM$_{10}$ and PM$_1$ at the high altitude Himalayan station Nepal Climate Observatory-Pyramid (NCO-P) (5079m a.s.l.). Atmos. Chem. Phys. 10, 4583–4596.

Dentener, F.J., Crutzen, P.J., 1994. A three-dimensional model of the globalammonia cycle. J. Atmos. Chem. 19 (4), 331–369.

Duchi, R., Cristofanelli, P., Marinoni, A., Bourcier, L., Laj, P., Calzolari, F., Adhikari, B., Verza, G.P., Vuillermoz, E., Bonasoni, P., 2014. Synoptic-scale dust transport events in the southern Himalaya. Aeolian Res. 13, 51–57.

EMEP Laboratory Intercomparison. Available at: http://www.nilu.no/projects/ccc/intercomparison/index.html (last access: 26.02.16.).

Fowler, D., Pilegaard, K., Sutton, M.A., Ambus, P., Raivonen, M., Duyzer, J., et al., 2009. Atmospheric composition change: ecosystems–atmosphere interactions. Atmos. Environ. 43, 5193–5267.

Galloway, J.N., Keene, W.C., Artz, R.S., Miller, J.M., Church, T.M., Knap, A.H., 1989. Processes controlling the concentrations of SO$_4^-$, NO$_3^-$, NH$_4^+$, H$^+$, HCOO$_T$ and CH3COO$_T$ in precipitation on Bermuda. Tellus 41B, 427–443.

Galy-Lacaux, C., Laouali, D., Descroix, L., Gobron, N., Liousse, C., 2009. Long term precipitation chemistry and wet deposition in a remote dry savanna site in Africa (Niger). Atmos. Chem. Phys. 9, 1579–1595.

Gupta, S.K., Deshpande, R.D., 2003. Synoptic hydrology of India from the data of isotopes in precipitation. Curr. Sci. 85 (11), 1591–1595.

Heath, J.A., Huebert, B.J., 1999. Cloudwater deposition as a source of fixed nitrogen in a Hawaiian montane forest. Biogeochemistry 44 (2), 119–134.

Heath, J., Baron, J.S., 2014. Climate, not atmospheric deposition, drives the biogeochemical mass-balance of a mountain watershed. Aquat. Geochem. 20 (2–3), 167–181.

Helsel, D.R., Hirsch, R.M., 2002. Statistical Methods in Water Resources Techniques of Water Resources Investigations. Book 4, chapter A3. U.S. Geological Survey. 522 pages.

Immerzeel, W.W., van Beek, L.P.H., Bierkens, M.F.P., 2010. Climate change will affect the Asian water towers. Science 328, 1382–1385.

Jeelani, Gh, Saravana Kumar, U., Kumar, Bhishm, 2013. Variation of $^\delta$18O and $^\delta$D in precipitation and stream waters across the Kashmir Himalaya (India) to distinguish and estimate the seasonal sources of stream flow. J. Hydrol. 481, 157–165.

Jenkins, M.D., Drever, J.I., Reider, R.G., Buchanan, T., 1987. Chemical composition of fresh snow on Mount Everest. J. Geophys. Res. 92 (D9), 10999–11002.

Kang, S., Mayewski, P.A., Qin, D., Yan, Y., Zhang, D., Hou, S., Ren, J., 2002. Twentieth century increase of atmospheric ammonia recorded in Mt. Everest ice core. J. Geophys. Res. 107 (D20), 4595. http://dx.doi.org/10.1029/2001JD001413.

Keene, W.C., Pszenny, A.A.P., Galloway, J.N., Hawley, M.E., 1986. Sea-salt corrections and interpretation of constituent ratios in marine precipitation. J. Geophys. Res. Atmos. 91, 6647–6658. http://dx.doi.org/10.1029/Jd091id06p06647.

Klimont, Z., Smith, S.J., Cofala, J., 2013. The last decade of global anthropogenic sulfur dioxide: 2000–2011 emissions. Environ. Res. Lett. 8 (1) p.014003.

Kumar, U.S., Kumar, B., Rai, S.P., Sharma, S., 2010. Stable isotope ratios in precipitation and their relationship with meteorological conditions in the Kumaon Himalaya, India. J. Hydrol. 391, 1–8.

Kurokawa, J., Ohara, T., Morikawa, T., Hanayama, S., Janssens-Manenhout, G., Fukui, T., Kawashima, K., Akimoto, H., 2013. Emissions of air pollutants and greenhouse gases over Asian regions during 2000–2008: regional emission inventory in ASia (REAS) version 2. Atmos. Chem. Phys. 13, 11019–11058.

Li, C., Kang, S., Zhang, Q., Kaspari, S., 2007. Major ionic composition of precipitation in the Nam Co region, central Tibetan Plateau. Atmos. Res. 85, 351–360.

Liu, Y.W., Xu-Ri, Wang, Y.S., Pan, Y.P., Piao, S.L., 2015. Wet deposition of atmospheric inorganic nitrogen at five remote sites in the Tibetan Plateau. Atmos. Chem. Phys. 15, 11683–11700.

Liu, B., Kang, S., Sun, J., Zhang, Y., Xu, R., Wang, Y., Liu, Y., Cong, Z., 2013. Wet precipitation chemistry at a high altitude site (3,326 m a.s.l.) in the southeastern Tibetan Plateau. Environ. Sci. Pollut. Res. 20, 5013–5027.

Marchetto, A., Arisci, S., Tartari, G.A., Balestrini, R., Tait, D., 2014. Stato ed evoluzione temporale della composizione chimica delle deposizioni atmosferiche nelle aree forestali della rete CONECOFOR. Forest@ − J. Silvic. For. Ecol. 11 (2), 72–85. http://dx.doi.org/10.3832/efor1003-011. http://www.sisef.it/forest@/contents/?id=efor1003-011.

Marinoni, A., Polesello, S., Smiraglia, C., Valsecchi, S., 2001. Chemical composition of fresh snow samples from the southern slope of Mt. Everest region (Khumbu–Himal region, Nepal). Atmos. Environ. 35, 3183–3190.

Marinoni, A., Cristofanelli, P., Laj, P., Duchi, R., Calzolari, F., Decesari, S., Sellegri, K., Vuillermoz, E., Verza, G.P., Villani, P., Bonasoni, P., 2010. Aerosol mass and black carbon concentrations, a twoyear record at NCO-P (5079 m, Southern Himalayas). Atmos. Chem. Phys. 10, 8551–8562.

Marinoni, A., Cristofanelli, P., Laj, P., Duchi, R., Putero, D., Calzolari, F., Landi, T.C., Vuillermoz, E., Maione, M., Bonasoni, P., 2013. High ozone and black carbon concentrations during pollution transport in the Himalayas: five years of continuous observations at NCO-P global GAW station. J. Environ. Sci. 25, 1618–1625.

Mittermeier, R.A., Gil, P.R., Hoffmann, M., Pilgrim, J., Brooks, T., Goettsch Mittermeier, C., Lamoreux, J., da Fonseca, G.A.B., 2005. Hotspots Revisited: Earth's Biologically Richest and Most Threatened Terrestrial Ecoregions. Mexico CEMEX Conservation International.

Nanus, L., Clow, D.W., Saros, J.E., Stephens, V.C., Campbell, D.H., 2012. Mapping critical loads of nitrogen deposition for aquatic ecosystems in the Rocky Mountains, USA. Environ. Pollut. 166, 125–135.

Palazzi, E., von Hardenberg, J., Provenzale, A., 2013. Precipitation in the Hindu-Kush Karakoram Himalaya: observations and future scenarios. J. Geophys. Res. Atmos. 118, 85–100.

Pauliquevis, T., Lara, L.L., Antunes, M.L., Artaxo, P., 2012. Aerosol and precipitation chemistry measurements vin a remote site in Central Amazonia: the role of biogenic contribution. Atmos. Chem. Phys. 12, 4987–5015.

Posch, M., Kamari, J., Forsius, M., Henriksen, A., Wilander, A., 1997. Exceedance of critical loads for lakes in Finland, Norway, and Sweden: reduction requirements for acidifying nitrogen and sulfur deposition. Environ. Manag. 21, 291–304.

Rozanski, K., Araguás-Araguás, L., Gonfiantini, R., 1993. Isotopic patterns in modern global precipitation. In: Swart, P.K., Lohmann, K.C., McKenzie, J., Savin, S. (Eds.), Climate Change Incontinental Isotopic Records. AGU, Washington, D. C, pp. 1–36. Geophys. Monogr. Ser.

Salerno, F., Guyennon, N., Thakuri, S., Viviano, G., Romano, E., Vuillermoz, E., Cristofanelli, P., Stocchi, P., Agrillo, G., Ma, Y., Tartari, G., 2015. Weak precipitation, warm winters and springs impact glaciers of south slopes of Mt. Everest (central Himalaya) in the last 2 decades (1994–2013). Cryosphere 9, 1229–1247.

Schiemann, R., Luthi, D., Schar, C., 2009. Seasonality and Interannual variability of the westerly Jet in the Tibetan Plateau region. J. Clim. 22, 2940–2957.

Sengupta, S., Sarkar, A., 2006. Stable isotope evidence of dual (Arabian Sea and Bay of Bengal) vapour sources in monsoonal precipitation over north India. Earth. Planet. Sci. Lett. 250, 511–521.

Shrestha, A.B., Wake, C.P., Dibb, J.E., Whitlow, S.I., 2002. Aerosol and precipitation chemistry at a remote Himalayan site in Nepal. Aerosol. Sci. Tech. 36, 441–456.

Sprenger, M., Wernli, H., 2015. The Lagrangian analysis tool LAGRANTO − version 2.0. Geosci. Model. Dev. 8, 2569–2586.

Tripathee, L., Kang, S., Huang, J., Sillanpää, M., Sharma, C.M., Lüthi, Z.L., Guo, J., Paudyal, K., 2014. Ionic composition of wet precipitation over the southern slope of central Himalayas. Nepal. Environ. Sci. Pollut. Res. 21, 2677–2687.

UNEP [United Nations Environment Programme], WCMC [World Conservation Monitoring Centre], 2008. Sagarmatha National Park, Nepal. In: McGinley, M., Cleveland, C.J. (Eds.), Encyclopedia of Earth. Environmental Information Coalition, National Council for Science and the Environment, Washington, DC.

Valsecchi, S., Smiraglia, C., Tartari, G., Polesello, S., 1999. Chemical composition of monsoon deposition in the Everest region. Sci. Total Environ. 226, 187–199.

Vet, R., Artz, R.S., Carou, S., Shaw, M., Ro, Chul-Un, Aas, W., Baker, A., Bowersox, V.C., Dentener, F., Galy-Lacaux, C., Hou, A., Pienaar, J.J., Gillett, R., Forti, M.C., Gromov, S., Hara, H., Khodzher, T., Mahowald, N.M., Nickovic, S., Rao, P.S.P., Reid, N.W., 2014. A global assessment of precipitation chemistry and deposition of sulfur, nitrogen, sea salt, base cations, organic acids, acidity and pH, and phosphorus. Atmos. Environ. 93, 3—100.

Walker, J.T., Aneja, V.P., Dickey, D.A., 2000. Atmospheric transport and wet deposition of ammonium in North Carolina. Atmos. Environ. 34, 3407—3418.

Wang, X., Zhang, L., Moran, M.D., 2014. Development of a new semi-empirical parameterization for below-cloud scavenging of size-resolved aerosol particles by both rain and snow. Geosci. Model. Dev. 7, 799—819.

Wayne, R.P., 1991. Chemistry of the Atmospheres, second ed. Clarendon Press, Oxford.

Wernli, H., Davies, H.C., 1997. A Lagrangian-based analysis of extratropical cyclones. I: the method and some applications. Q. J. Roy. Meteor. Soc. 123, 467—489.

Williams, M.W., Seibold, C., Chowanski, K., 2009. Storage and release of solutes from a subalpine seasonal snowpack: soil and stream water response, Niwot Ridge, Colorado. Biogeochemistry 95, 77—94.

WMO-GAW Inter-Laboratory Comparison Study. Available at: www.qasac-americas. org. (last access: 26.02.14.).

Xu, B.-Q., Wang, M., Joswiak, D.R., Cao, J.-J., Yao, T.-D., Wu, G.-J., Yang, W., Zhao, H.-B., 2009. Deposition of anthropogenic aerosols in a southeastern Tibetan glacier. J. Geophys. Res. 114, D17209. http://dx.doi.org/10.1029/2008JD011510.

Yao, T.D., Thompson, L., Yang, W., Yu, W., Gao, Y., Guo, X., Yang, X., Duan, K., Zhao, H., Xu, B., Pu, J., Lu, A., Xiang, Y., Kattel, D.B., Joswiak, D., 2012. Different glacier status with atmospheric circulations in Tibetan Plateau and surroundings. Nat. Clim. Change 2 (9), 663—667.

Zhang, D.D., Peart, M., Jim, C.Y., He, Y.Q., Li, B.S., Chen, J.A., 2003. Precipitation chemistry of Lhasa and other remote towns. Tibet. Atmos. Environ. 37, 231—240.

Zhao, S., Ming, J., Sun, J., Xiao, C., 2013. Observation of carbonaceous aerosols during 2006—2009 in Nyainqentanglha mountains and the implications for glaciers. Environ. Sci. Poll. Res. 20, 5827—5838.